Engineering Notes

ENGINEERING NOTES are short manuscripts describing new developments or important results of a preliminary nature. These Notes cannot exceed 6 manuscript pages and 3 figures; a page of text may be substituted for a figure or vice versa. After informal review by the editors, they may be published within a few months of the date of receipt. Style requirements are the same as for regular contributions (see inside back cover).

Further Consideration of "Spilled" Leading-Edge Vortex Effects on Dynamic Stall

Lars E. Ericsson* and J. Peter Reding†
Lockheed Missiles & Space Company, Inc., Sunnyvale, Calif.

Introduction

IT has been shown in an earlier Note[1] how the quasisteady engineering analysis methods of Ref. 2 can be extended to include the transient effects of the "spilled" leading-edge vortex. The present Engineering Note shows how this provides good prediction of experimental results obtained in large-amplitude oscillations in pitch[3,4] and fast rampwise changes of angle of attack.[5‡]

Discussion

It was shown in Ref. 1 that the phase characteristics measured by McCroskey et al.[4] for Begin of Stall and Moment Maximum could be predicted very well. However, the corresponding moment amplitude was underpredicted. The likely reason for this is the following. At least for the popular NACA-0012 airfoil, static data[7] show a prestall loss of lift (Fig. 1). This is caused by trailing-edge separation, which does not have time to develop in the case of dynamic stall because of the additional convective time lag associated with trailing-edge stall.[2] Thus, Δc^*_{lv} rather than Δc_{lv} should be used (see inset in Fig. 2). The variation of the ratio $\Delta c^*_{lv}/\Delta c_{lv}$ with Reynolds number obtained from Fig. 1 for NACA-0012 is shown in Fig. 2. The infinite Reynolds number asymptote applicable to the dynamic stall case[2] gives $\Delta c^*_{lv}/\Delta c_{lv} = 1.5$. Thus, for the NACA-0012 airfoil, the vortex-induced lift derived in Ref. 1 should be increased by 50%, giving

$$\Delta c_{nv} = 1.5\pi \sin^2 \alpha_{vs} \tag{1}$$

where α_{vs} is the dynamic stall angle, including the effect of the moving separation point.[1,2] Combining Eq. (1) with the analysis of Ref. 8 gives the following simple result for the common case that the pitch axis is located at 25% chord.

$$(c_{n\max})_{\rm dyn} = (c_{n\max})_{Re\to\infty} + \Delta c_{nv} \tag{2a}$$

$$-(c_{m\max})_{\rm dyn} = \Delta c_{ms} + \Delta c_{nv} \tag{2b}$$

Δc_{ms} is the quasisteady value for the moment change at dynamic stall.[8] Figure 3 is Fig. 19 of Ref. 3, in which the present prediction through Eqs. (1) and (2) has been added. The figure shows good agreement between experimental results[4] and present prediction.

Presented at the AIAA 3rd Atmospheric Flight Mechanics Conference, Arlington, Texas, June 7-9, 1976 (in bound volume of Conference papers; no paper number); submitted Sept. 3, 1976.
Index categories: Aerodynamics; Nonsteady Aerodynamics.
*Consulting Engineer. Asociate Fellow AIAA.
†Research Specialist. Member AIAA.
‡The present Engineering Note, together with Ref. 1, is contained essentially in Ref. 6.

Rampwise α-Change

In the case of rampwise α-change, α_{vs} is composed as follows.[2]

$$\alpha_{vs} = \alpha_s + \Delta\alpha_w + \Delta\alpha_s + \Delta\alpha_{sp} \tag{3a}$$

$$\Delta\alpha_w = \xi_w c\dot{\alpha}/U_\infty \tag{3b}$$

$$\Delta\alpha_s = K_a c\dot{\alpha}/U_\infty \tag{3c}$$

$$\Delta\alpha_{sp} = \xi_{sp} c\dot{\alpha}/U_\infty \tag{3d}$$

For the turbulent-type leading-edge stall occurring on most airfoils,[3,4] the following parameter values apply in Eq. (3).

$$\xi_w = 1.5 \tag{4a}$$

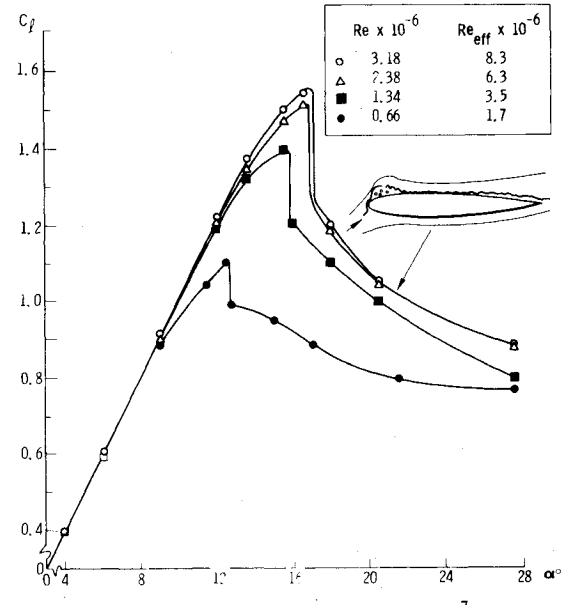

Fig. 1 Section lift of NACA 0012.[7]

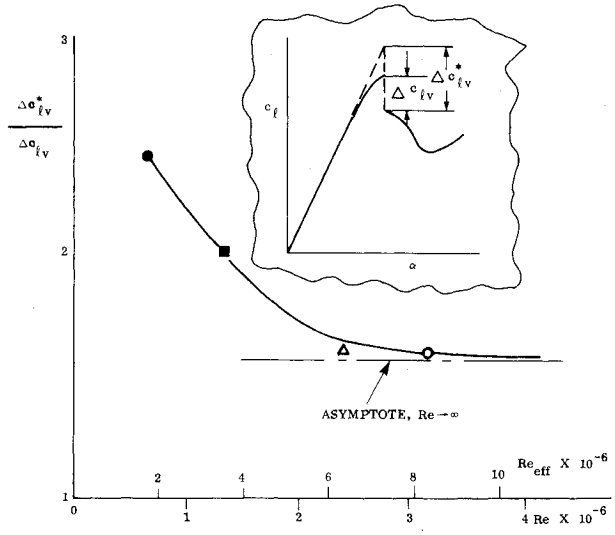

Fig. 2 Linear overshoot of stall.

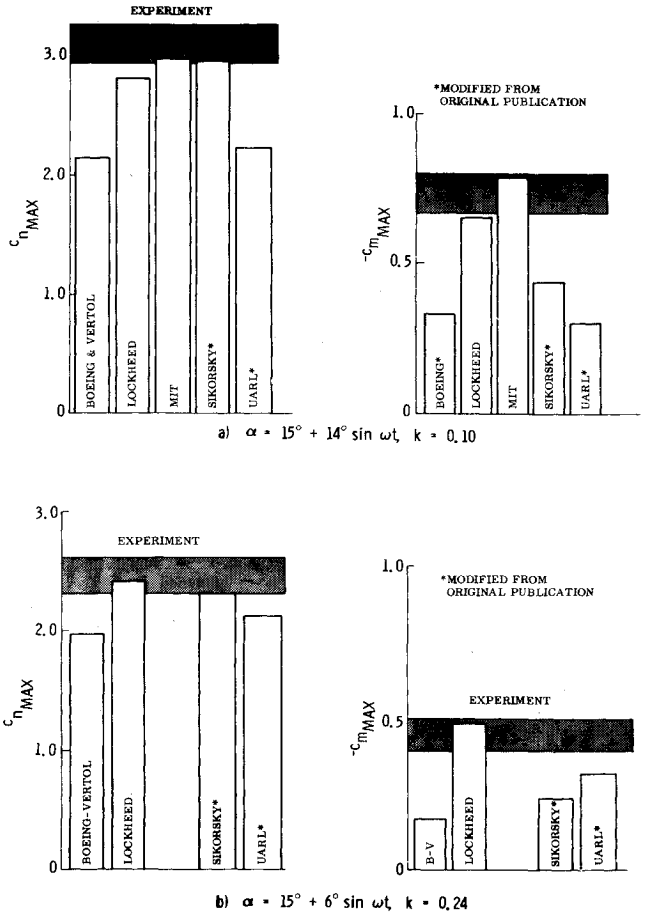

Fig. 3 Predictions and measurements of maximum normal force and pitching moment coefficients for an oscillating NACA 0012 airfoil.

$$K_a = 2(I + 2\xi_{cg}) \tag{4b}$$

$$\xi_{sp} = 0.75 \tag{4c}$$

The experimental results obtained by Ham et al.[5] are plotted in Fig. 4, together with the angle-of-attack variation with time. The angular rate can be approximated by two constant values: a slow rate of $c\dot{\alpha}_1/U_\infty = 0.012$ below $\alpha_1 = 5°$, and a much higher rate, $c\dot{\alpha}_2/U_\infty = 0.043$, for $\alpha > 5°$. At $\alpha = 5°$ the flow is attached, and the total time lag before the new rate can influence the lift is simply the Kármán-Sears lag,[8,9] viz., $\Delta_{s2} = 1.5\ c\dot{\alpha}_2/U_\infty = 3.7°$. Adding this time lag effect to $\alpha_1 = 5°$ gives the angle of attack, $\alpha_2 = 8.7°$, at which the higher angular rate starts affecting the aerodynamic characteristics. Because of pitch-rate-induced camber and apparent mass effects, the attached flow lift curve will lag the static lift by only half of the Kármán-Sears wake lag.[2] Thus, the lag is $\Delta\alpha_{w1}/2 = 0.5°$ for $\alpha < \alpha_2$ and $\Delta\alpha_{w2}/2 = 1.9°$ for $\alpha > \alpha_2$. To this attached flow lift is added the "spilled" vortex effect, Eq. (1), as described in Ref. 1. The resulting predicted lift is shown by the solid line in Fig. 4. It appears that, aside from an α-zero shift of 2.5° (in the apparent static reference data), the attached-flow lift characteristics are in good agreement with experimental results.[5] Applying this α-zero shift in the present analysis gives the predicted lift and moment characteristics shown in Fig. 5. The agreement between prediction and experimental results[5] is rather good. In regard to the differences, the following can be said.

Three-dimensional flow phenomena can distort the "two-dimensional" measurements made in one chordwise strip using fast-response pressure transducers, as in the present case.[10] The α-zero shift could have been caused by such interference effects. Less likely is that it, as well as the deviation

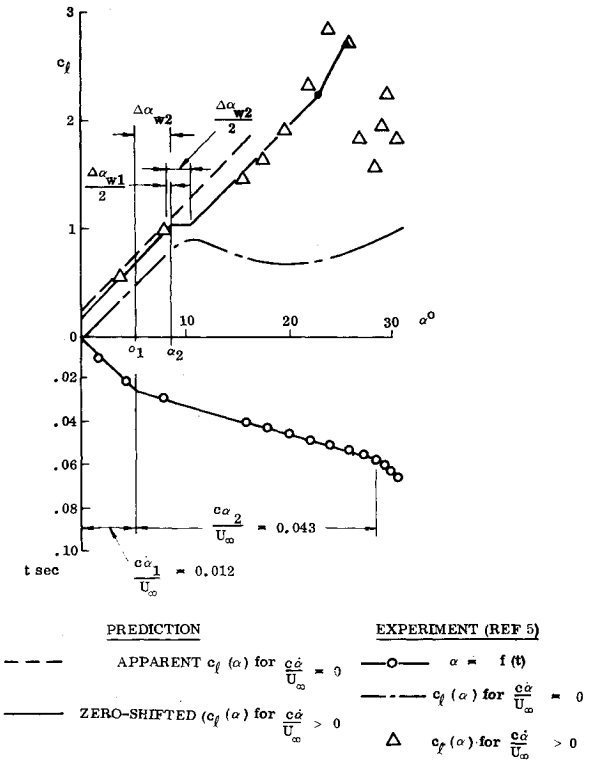

Fig. 4 Nonlinear α-ramp characteristics.

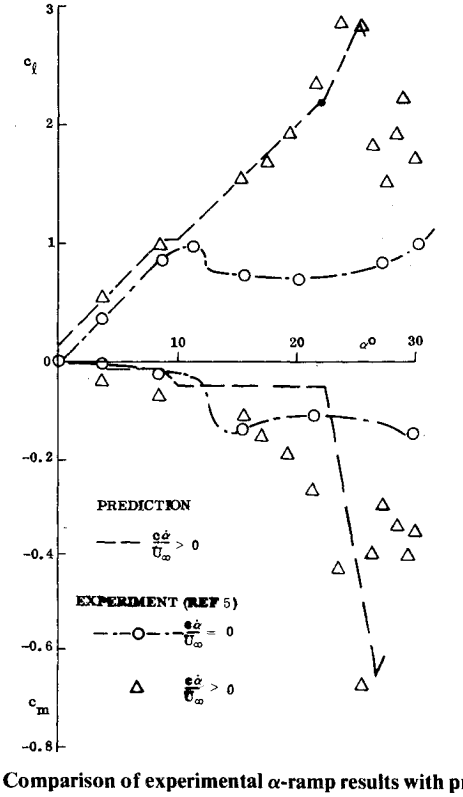

Fig. 5 Comparison of experimental α-ramp results with predictions.

between static and dynamic substall moment characteristics, could have been introduced electronically during data recording and processing. Moss and Murdin,[11] who performed almost the same experiment as Ham and Garelick,[5] conclude that their anomalous dynamic results were caused in large part by three-dimensional flow distortion. McCroskey et al.[4] observed in their test "large three-dimensional in-

teractions between the model and the tunnel-wall boundary layers" but found the effects to be decreasing with increasing frequency until they were effectively filtered out and "could hardly be detected for $k>0.15$." Thus, the high-frequency results ($\bar{\omega}\geq 0.3$) in Fig. 3 are free from three-dimensional flow-interference effects. However, the lower-frequency results in Fig. 3, as well as the α-ramp data in Figs. 4 and 5, presumably all can have been influenced by three dimensional flow inteference.

Conclusions

It has been shown in the present Note and Ref. 1 how a previously developed quasisteady theory for dynamic stall[2] can be extended to include the transient effects of the "spilled" leading edge vortex. The more important results are as follows.

1) Adding the moving separation point effect to the quasisteady separation value correctly predicts the "spilling" of the leading-edge vortex.

2) The travel of the "spilled" leading-edge vortex over the chord occurs at 55% of freestream speed. Peak pitching moment values occur shortly before the "spilled" vortex leaves the trailing edge, and peak normal force occurs when the vortex is at 70% chord.

3) By the use of Polhamus' leading-edge suction analogy, a simple means is provided for prediction of the loads induced by the "spilled" vortex.

The present analytic method correctly predicts the large "spilled" vortex effect measured in high-amplitude oscillations in pitch. Furthermore, the developed analytic means predict the very nonlinear characteristics for rampwise change of angle of attack observed by Ham et al. (when due consideration is taken of the experimental accuracy). These results all indicate that the present analytic method could be applied to predict the nonlinear, nonharmonic unsteady characteristics of a helicopter blade passing through the stall region.

References

[1]Ericsson, L. E. and Reding, J. P., " 'Spilled' Leading Edge Vortex Effects on Dynamic Stall Characteristics," *Journal of Aircraft,* Vol. 13, April 1976, pp. 313-315.

[2]Ericsson L. E. and Reding, J. P., "Dynamic Stall Analysis in Light of Recent Numerical and Experimental Results," *Journal of Aircraft,* Vol. 13, April 1976, pp. 248-255; also AIAA Paper 75-26.

[3]McCroskey, W. J., "Recent Developments in Dynamic Stall," *Symposium on Unsteady Aerodynamics,* University of Arizona, Tucson, Ariz., March 18-20, 1975.

[4]McCroskey, W. J., Carr, L. W., and McAllister, K. W., "Dynamic Stall Experiments on Oscillating Airfoils," *AIAA Journal,* Vol. 14, Jan. 1976, pp. 57-63.

[5]Ham, N. D. and Garelick, M. S., "Dynamic Stall Considerations in Helicopter Rotors," *American Helicopter Society Journal,* Vol. 13, April 1968, pp. 44-55.

[6]Ericsson, L. E. and Reding, J. P., "Dynamic Stall Reconsiderations," *Proceedings AIAA 3rd Atmospheric Flight Mechanics Conference,* Arlington, Texas, June 7-9, 1976, pp. 70-78.

[7]Jacobs, E. N. and Sherman, A., "Airfoil Section Characteristics as Affected by Variations in the Reynolds Number," NACA TR 586, 1937.

[8]Ericsson, L. E. and Reding, J. P., "Unsteady Airfoil Stall, Review and Extension," *Journal of Aircraft,* Vol. 8, Aug. 1971, pp. 609-616.

[9]Von Kármán, T. and Sears, W. R., "Airfoil Theory for Non-Uniform Motion," *Journal of the Aeronautical Sciences,* Vol. 5, Aug. 1938, pp. 379-390.

[10]Ericsson, L. E. and Reding, J. P., "Dynamic Stall Stimulation Problems," *Journal of Aircraft,* Vol.8, July 1971, pp. 579-583.

[11]Moss, G. F. and Murdin, P. M., "Two-Dimensional Low-Speed Tunnel Tests on the NACA 0012 Section Including Measurements Made During Pitch Oscillations at the Stall," Aeronautical Research Council, Great Britain, C P 1145, 1971.

Bodies of Revolution with Wavy Afterbodies at Large Incidences

V. S. Holla* and B. S. Varambally†
Indian Institute of Science, Bangalore, India

Introduction

ROCKET and missile shapes, during flight, usually deform both longitudinally and circumferentially because of the aerodynamic loads acting on the flexible structure. A knowledge of the aerodynamic forces and moments on these deformed shapes is important from both stability as well as aeroelastic viewpoints. At low incidence one can use the well-known slender-body theory to calculate the normal force and pitching moment, and it may very well turn out that changes in these quantities caused by body deformation are negligibly small. However, at large incidences, because of viscous crossflow separation, the effect of body deformation on the normal force, moment, and center of pressure may not be negligible. In the present Note the effect of body deformation in the form of longitudinal waviness along the afterbody on the normal force, moment, and center of pressure is considered under the conditions of laminar flow at subcritical Reynolds numbers.

Analysis

The well-known simple method to estimate the total normal force C_N, pitching moment C_M coefficients on slender bodies at large incidence is to superimpose the results from slender-body theory for linear parts (C_{N1}, C_{M1}) and a proper crossflow theory for nonlinear parts (C_{N2}, C_{M2}) of C_N and C_M. Allen's[1] crossflow drag concept as extended by Kelly[2] (using the impulsive flow analogy) is used here to calculate the C_{N2} and C_{M2}. Using Sarpakaya's (Fig. 6, Ref. 3) experimental results, the crossflow drag variation along the body is represented by

$$C_{D_c}(x)=\sum_{1}^{6} a_n\left\{\frac{x\tan\alpha}{r(x)}\right\}^n \tag{1}$$

The a_n's, obtained by a curve-fitting procedure, are given by: $a_1=0.4632$, $a_2=-0.48295\times10^{-1}$, $a_3=0.20405\times10^{-2}$, $a_4=-0.20392\times10^{-4}$, $a_5=-0.23214\times10^{-6}$, and $a_6=0.707475\times10^{-8}$. Next, the cross-sectional radius of a body with power law ogival nose and wavy afterbody shape can be written as

$$r(x)=R_B(x/H)^p \qquad 0\leq x\leq H$$

$$r(x)=R_B+\delta\sin[(x-H)N\pi/(L-H)] \qquad H\leq x\leq L \tag{2}$$

where N is the number of half-waves and δ is the amplitude (Fig. 1). For this wavy body, the linear parts of normal force and moment coefficients C_{N1W} and C_{M1W} are obtained, using the slender-body theory of Munk and Ward, to give

$$C_{N1W}=\sin2\alpha\cdot\cos(\alpha/2) \tag{3}$$

$$C_{M1W}=[V-S_B(L-X_m)]\sin2\alpha\cos(\alpha/2)/S_B\cdot D_B \tag{4}$$

where V, the volume of the body, is given by

$$V=[\pi R_B^2H/(2p+1)]+\pi R_B^2(L-H)+\pi\delta^2(L-H)/2$$
$$+2\delta R_B(L-H)(1-\cos N\pi)/N \tag{5}$$

Received Oct. 21, 1976; revision received Jan. 5, 1977.

Index categories: Aerodynamics; LV/M Aerodynamics; Jets, Wakes, and Viscid-Inviscid Flow Interactions.

*Assistant Professor.

†Aerodynamics Engineer, VSSC Trivendrum, India.